

Superconducting fluctuation effects on the electron spin susceptibility in $\text{YBa}_2\text{Cu}_3\text{O}_{6.95}$

H. N. Bachman, V. F. Mitrović, A. P. Reyes,* W. P. Halperin, M. Eschrig, and J. A. Sauls

Department of Physics and Astronomy, and Science and Technology Center for Superconductivity, Northwestern University, Evanston, Illinois 60208

A. Kleinhammes,† P. Kuhns, and W. G. Moulton

National High Magnetic Field Laboratory, Tallahassee, Florida 32310

(Received 10 February 1999)

The electronic spin susceptibility of $\text{YBa}_2\text{Cu}_3\text{O}_{6.95}$ has been measured with high precision up to 24 T with ^{17}O nuclear magnetic resonance. Its temperature dependence can be accounted for by superconducting fluctuations that result in a smooth crossover from the normal to the vortex liquid state. A magnetic-field-temperature phase diagram for this crossover has been established having strong upward curvature. [S0163-1829(99)06033-6]

The upper critical field is large in high- T_c materials because of their small superconducting coherence lengths. However, a precise determination of $H_{c2}(T)$ at high magnetic fields is difficult because there is no well-defined signature of a phase transition. In magnetic fields significantly larger than the lower critical field [$H_{c1}(0) \approx 100$ G] the transition is broadened by the opening of a pseudogap in the electronic excitation spectrum. We performed a detailed experimental and theoretical study of the fluctuation effects on the spin susceptibility in optimally doped $\text{YBa}_2\text{Cu}_3\text{O}_{6.95}$ (YBCO) and developed a quantitative understanding for the onset of superconductivity solely in terms of a pairing pseudogap. This allows us to define a crossover field, $H_{c2}(T)$, up to high magnetic fields.

In high- T_c materials the effects of a magnetic field on pairing fluctuations have been discussed for the diamagnetic response,^{1,2} resistivity,³ and heat capacity.⁴ In general, efforts to determine $H_{c2}(T)$ have relied on *ad hoc* criteria that are not related to superconducting fluctuations. The specific heat has been analyzed by Roulin *et al.*⁴ using several criteria to determine $H_{c2}(T)$. Magnetization measurements of Welp *et al.*¹ show rounding in $M(T)$ near the expected transition temperature as the field is increased. In this case the transition temperature was determined by linear extrapolation of the temperature-dependent diamagnetism in the superconducting state to intersect with the normal-state magnetization.

In the present work we determine $H_{c2}(T)$ from measurements of the Pauli spin susceptibility, χ_s . We measure the ^{17}O nuclear-magnetic-resonance (NMR) Knight shift and isolate the contribution of χ_s , taking into account orbital, diamagnetic, and vortex shifts. Because of the high precision of ^{17}O NMR, we measure the temperature dependence of χ_s to better than 0.1% of the total normal-state χ_s value. Thus, we are able to make a quantitative comparison of the data with the theory of pairing fluctuation corrections to χ_s in the normal state. In the superconducting state there is a mean-field region where χ_s is linear in temperature. A crossing-point analysis defines the crossover temperature, $T_c(H)$. We performed this analysis in magnetic fields up to 24 T.

Our aligned powder sample is the same as that studied

previously^{5,6} having 30–40% ^{17}O -enriched $\text{YBa}_2\text{Cu}_3\text{O}_{6.95}$ prepared by solid-state reaction. Low-field magnetization data show a sharp T_c at 92.5 K. The ^{17}O NMR spectra were obtained from the fast Fourier transform of a Hahn echo sequence: $\pi/2$ - τ - π -acquire and only the ($1/2 \leftrightarrow -1/2$) transition of the O(2,3) sites was studied. High rf power allowed the use of short ($\approx 1.5 \mu\text{s}$) $\pi/2$ pulses ($2.5 \mu\text{s}$ at 2.1 T), giving a useful bandwidth > 100 kHz. The $^{17}\text{O}(2,3)$ ($1/2 \leftrightarrow -1/2$) resonance has a low-frequency tail owing to oxygen deficiency in a small portion of the sample.⁵ Its effect on our measurements was eliminated by performing a non-linear least-squares fit in the frequency domain that isolates the dominant, narrow spectrum of optimally doped YBCO. Temperature stability was ± 0.1 K or better. For $H_0 \leq 14.9$ T we used superconducting magnets. The shifts measured at 8.4 T were the most precise. The high-field measurements, 18.7 T to 24 T, were performed in a Bitter magnet adapted for modest homogeneity NMR at the National High Magnetic Field Laboratory in Tallahassee, Florida. High-voltage arcing and temperature stability in the constrained space of the Bitter magnet required that we design a special probe.⁷

Excluding temperature-independent quadrupolar terms, the frequency of ^{17}O NMR in YBCO can be written,

$$\nu = {}^{17}\gamma[H_0(1 + {}^{17}K_{\text{spin}} + {}^{17}K_{\text{orb}}) + \Delta H_{\text{dia}} + \Delta H_{\text{v}}].$$

The gyromagnetic ratio of ^{17}O is ${}^{17}\gamma$; H_0 is the static magnetic field applied parallel to the \hat{c} axis; ΔH_{v} is a spatially varying field that results from pinned vortices, appearing below the melting or pinning temperature.⁵ The orbital shift, ${}^{17}K_{\text{orb}}$, is small and temperature independent. The diamagnetic contributions, ΔH_{dia} , whose origin is from surface supercurrents, are negligible at large fields.⁶ In the vortex liquid state the inhomogeneous vortex fields, ΔH_{v} , are motionally averaged. At low temperatures vortices are pinned, and the resonance for ^{17}O nuclei in their vicinity is shifted to lower frequencies by ${}^{17}\gamma\Delta H_{\text{v}}$ compared to nuclei in the vortex liquid phase. This shift allows us to identify the ^{17}O resonance associated with the vortex liquid.⁵ The temperature dependence of this part of the spectrum is given by ${}^{17}K_{\text{spin}}$, which is proportional to the electron spin suscepti-

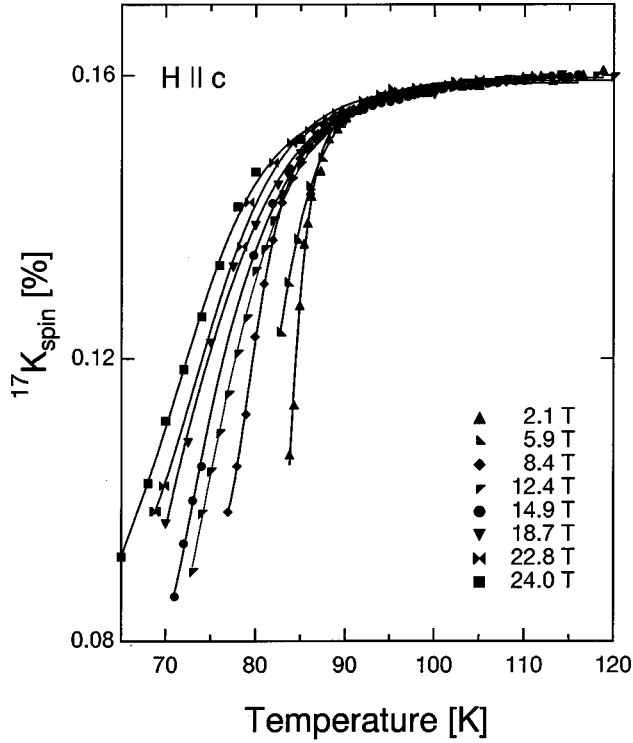


FIG. 1. The $^{17}\text{O}(2,3)$ spin shift at different magnetic fields for $\text{YBCO}_{6.95}$. The spin shift is proportional to the Pauli spin susceptibility. Lines are guides to the eye.

bility, χ_s . The high sensitivity of $^{17}\text{O}(2,3)$ NMR to χ_s , via the \hat{c} -axis hyperfine coupling, is an advantage compared with that of $^{63}\text{Cu}(2)$ where the \hat{c} -axis coupling is quite small and the copper resonance is broad.

In Fig. 1 we show the temperature-dependent shifts for $^{17}\text{O}(2,3)$ measured over a magnetic field range of 2.1 T to 24 T. The normal-state values at 120 K are fixed to the value of $^{17}K_{\text{spin}}$ in the normal state, $0.16\% \pm 0.01\%$. $^{17}K_{\text{spin}}$ is the percentage spin shift relative to the Larmor frequency of the ^{17}O nucleus and is attributable only to the electron spin susceptibility. The normal-state value is determined independently from the extrapolation to the high field of the difference $^{17}K(T=100\text{ K}) - ^{17}K(T=20\text{ K})$. This expression extrapolates to the normal state $^{17}K_{\text{spin}}$ because other contributions to the total spectrum shift are either negligible at high fields (ΔH_{dia} and ΔH_{v}), temperature independent ($^{17}K_{\text{orb}}$), or both (quadrupolar terms). The decrease of $^{17}K_{\text{spin}}$ with decreasing temperature is smooth, showing no discontinuities in either magnitude or slope, suggestive of a crossover region. The crossover shifts to lower temperatures as the field is increased.

Peak frequencies were determined by nonlinear least-squares fits to a Gaussian around the peak region. In our stable superconducting magnet (8.4 T) this method allowed us to achieve precision in determination of the peak frequency of one part per million, corresponding to better than one part in a thousand precision relative to the total normal-state value of $^{17}K_{\text{spin}}$. For data obtained with the Bitter magnet, corrections are required for variations of magnetic field with cooling water temperature, and thus the precision of the peak frequencies is only five parts per million. In Fig. 2(a)

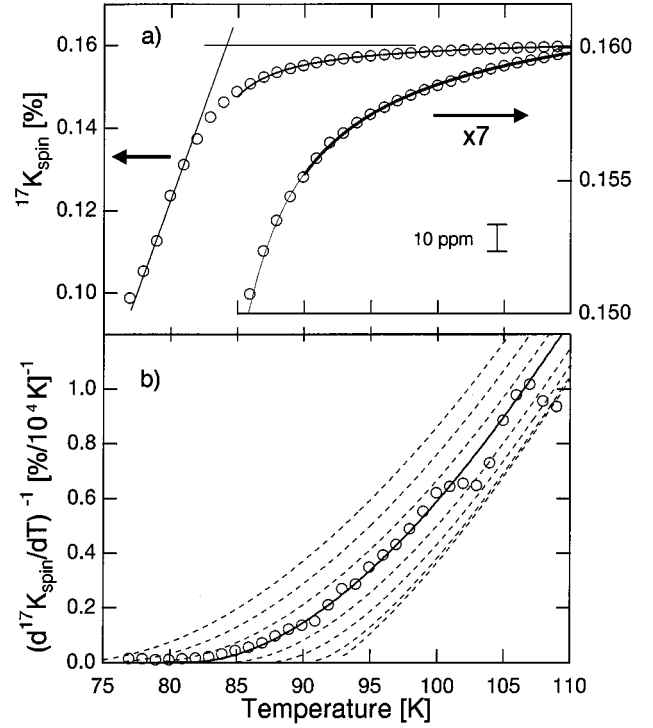


FIG. 2. $^{17}\text{O}(2,3)$ spin shift at 8.4 T for $H||\hat{c}$. The theoretical calculation taking into account two-dimensional (2D) pairing fluctuations is shown as curves. (a) The inset shows a factor of seven expanded vertical scale demonstrating excellent agreement between theory and experiment. The crossed lines determine T_c , as discussed in the text. (b) The inverse of the derivative, $(d^{17}K_{\text{spin}}/dT)^{-1}$, as discussed in the text. The dashed curves indicate calculations for $T_{\text{cmf}} = 72\text{ K}, 75\text{ K}, 78\text{ K}, 80.9\text{ K}, 84\text{ K}, 87\text{ K}, 90\text{ K}, 92.5\text{ K}$.

we plot $^{17}K_{\text{spin}}$ at 8.4 T with an expanded version in the inset but on the same temperature scale. The $^{17}K_{\text{spin}}$ data have a monotonic decrease easily discernible below 110 K.

The precision of our spin shift measurements at 8.4 T allows a quantitative comparison with the theory of superconducting fluctuations. Pairing fluctuation corrections to the Pauli spin susceptibility in the zero-field limit have been considered theoretically by several authors.^{8,9} Gaussian fluctuation corrections diverge at the mean-field transition temperature T_{cmf} . Calculations for fluctuation contributions to the spin susceptibility based on long wavelength static fluctuations at zero field near T_{cmf} predict $(d\delta\chi_s/dT)^{-1} \propto T - T_{\text{cmf}}$ in two dimensions,⁸ which cannot explain the curvature in our measurements shown in Fig. 2(b), and $(d\delta\chi_s/dT)^{-1} \propto \sqrt{T - T_{\text{cmf}}}$ in three dimensions,⁹ producing curvature opposite to that of our measurements.

We calculate χ_s in the weak-coupling limit for a quasi-two-dimensional, d -wave superconductor taking into account Landau quantization of the orbital motion of pairs by a magnetic field ($H||\hat{c}$). Our calculations include dynamical pairing fluctuations and we sum over all Landau levels in order to extend the range of validity of the theory to higher fields and temperatures. A detailed presentation of the theory is given in Eschrig *et al.*;¹¹ here we provide a short summary. The pair fluctuation propagator for d -wave pairing with coupling constant g is given by $L(Q)^{-1} = g^{-1}$

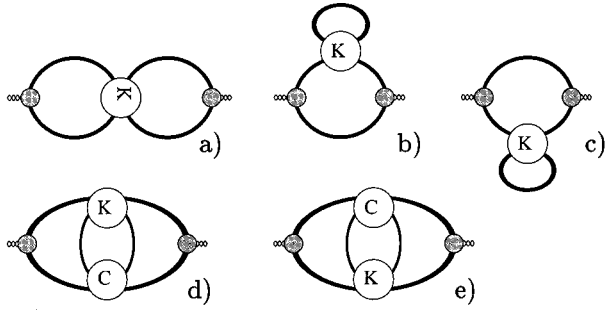


FIG. 3. Feynman diagrams for the pairing fluctuation corrections to the Pauli spin susceptibility, to leading order in T_{cmf}/E_F , as discussed in the text.

$-T\Sigma_{\epsilon_n} B_2(\epsilon_n, Q)$, where $B_2(\epsilon_n, Q)$ is an impurity renormalized two-particle susceptibility in the d -wave pairing channel as discussed in Mitrović *et al.*¹⁰ and in Eschrig *et al.*¹¹ We use the notation $Q = (\omega_l, \vec{q})$, which combines Matsubara energy, $\omega_l = 2\pi lT$, and pair momentum \vec{q} of the fluctuation mode; the latter is quantized in a magnetic field. The results we obtain derive from the summation of all leading order pairing fluctuation corrections in T_{cmf}/E_F (E_F is the Fermi energy renormalized by exchange field corrections), given by the diagrams shown in Figs. 3(a)–3(e), the Maki-Thompson (a), the density-of-states (b),(c), and the Aslamazov-Larkin (d),(e) contributions. K denotes the fluctuation propagator renormalized by external vertex corrections due to impurities. In contrast to the fluctuation corrections to the spin-lattice relaxation rate the contributions (d),(e) in Fig. 3 have the same order in T_{cmf}/E_F as (a)–(c). However, they contain only one singlet pair fluctuation mode K , the other mode in the particle-particle channel is a triplet impurity Cooperon-like mode C . In the clean limit diagrams (d),(e) vanish, in the dirty limit they give the main contribution. For intermediate impurity scattering all diagrams contribute significantly. It is possible to write the sum of all diagrams in Fig. 3 in a compact way. Considering $B_2(\epsilon_n, Q)$ as a functional of the quasiparticle impurity self-energy $\Sigma(\epsilon_n)$, the sum of all leading order pairing fluctuation corrections to χ_s can be written as¹¹

$$\delta\chi_s = (\gamma_e \hbar)^2 \sum_{n, Q} \frac{\delta^2 B_2(\epsilon_n, Q)}{\delta \Sigma(\epsilon_n)^2} L(Q). \quad (1)$$

In Fig. 2 our calculation for 8.4 T is compared with experiment. The parameters extracted from the fit yield $E_F = 930 \pm 30$ meV, and $T_{cmf} = 80.9 \pm 0.3$ K. We used the same scattering parameters as in our comparison of the theory of dynamical pairing fluctuations with the field dependence of spin-lattice relaxation in Mitrović *et al.*¹⁰ Dynamical fluctuations and orbital quantization effects produce the curvature shown in Fig. 2(b). The fit to our theory is performed in the region $T > 90$ K, and is shown by the heavy solid curve in Fig. 2(a). Extension of the same fit to lower temperatures, as indicated by the thin solid curve, demonstrates that the theory fits the data well down to $T = 85$ K. Below this temperature critical fluctuations become significant.

From the temperature dependence of the spin susceptibility in the mean-field regime of the superconducting state it is possible to extrapolate linearly back to the susceptibility of

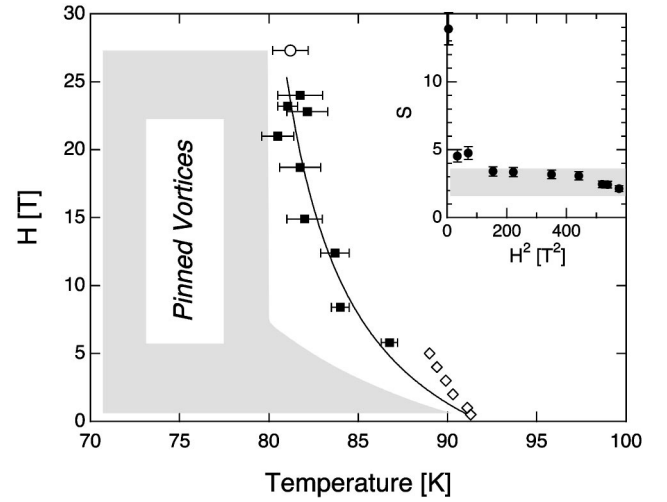


FIG. 4. H - T phase diagram from electron spin susceptibility as determined by ^{17}O NMR for $\text{YBCO}_{6.95}$. The dark squares represent a determination of $H_{c2}(T)$ as discussed in the text. The curve is a guide to the eye. Vortices become pinned in the cross-hatched region (Ref. 5) The open circle indicates the onset of vortex pinning, an extension of the earlier work of Bachman *et al.* (Ref. 5). Open diamonds are from diamagnetism measurements (Ref. 1). Inset: Magnetic-field dependence of $S = [d(^{17}K_{\text{spin}})/dT]_{\text{max}} \times [T_c / ^{17}K_{\text{spin}}(120\text{K})]$.

the normal state to determine a crossover temperature T_c . We determined the linear temperature dependence of the NMR spin shift in the superconducting state from the maximum slope, $d(^{17}K_{\text{spin}})/dT$, and performed an extrapolation to the normal-state shift of 0.16% to find T_c ; see Fig. 2(a). The results are presented in Fig. 4. In particular, at 8.4 T, we found $T_c = 84 \text{ K} \pm 0.5 \text{ K}$. The slopes we used are shown in the inset of Fig. 4 for various fields. Because the slope is expected to scale with Δ^2 , we can confirm the validity of our approach by comparing the slopes in Fig. 4 with direct measurements of the energy gap Δ . Tunneling and photoemission measurements¹² suggest a gap of $2\Delta/k_B T_c = 6 \pm 1$ for YBCO. Using the mean field result for χ_s without exchange corrections, but allowing for gap anisotropy, we estimate the scaled slope for d -wave pairing to be in the range 1.8–3.6, shown in the inset of Fig. 4 as a cross-hatched region. The anomalously large slope at 2.1 T can be attributed to diamagnetic contributions to the frequency shift measurement. For all other fields the experimental slopes presented in the inset of Fig. 4 are consistent with our expectation for the slope of χ_s . The crossover line $H_{c2}(T)$ in Fig. 4 exhibits upward curvature. Qualitatively similar behavior, but at lower fields, has been reported in specific-heat experiments.⁴ With decreasing temperature there is a smooth crossover from the fluctuation regime to a vortex liquid phase. Deviations of our theory from experiment in Fig. 2 below 85 K indicate the onset of critical fluctuations. The smooth crossover suggests a relationship between critical fluctuations and the vortex liquid phase. However, there is no adequate theory for the interplay between critical fluctuations and the fluctuating currents in the vortex liquid.

The vortex liquid phase becomes well established at temperatures less than those given by $H_{c2}(T)$. At lower temperatures vortices become pinned, as we have shown previously.⁵

Using two independent methods we determined a region of the phase diagram in which pinned vortices are present, which we show as the hatched region of Fig. 4. We have extended that work to 27.3 T, shown as an open circle in Fig. 4, where the onset of vortex pinning is observed by spin-spin relaxation. For low fields we point out that the pinning temperature and melting temperature^{3,4} of untwinned, single crystals coincide. Our understanding of vortex pinning in combination with our new measurements of $H_{c2}(T)$ show that the region of liquid vortex matter is restricted to both high temperatures and low magnetic fields.

In summary, we find that ^{17}O NMR Knight shifts give a precise determination of the temperature dependence of the Pauli spin susceptibility χ_s . We find significant rounding near T_c indicating that superconducting fluctuations smear the transition. Consequently, the transition is best represented as a crossover from normal-state behavior to that of a vortex liquid. Our calculations for superconducting fluctuations, taking into account dynamical pairing fluctuations and

the effects of orbital quantization, are in excellent agreement with experiment in the temperature range down to T_c . The decreasing susceptibility with decreasing temperature above T_c can be fully accounted for by the opening of a pairing pseudogap. Finally, we have established the $H_{c2}(T)$ phase diagram for $\text{YBa}_2\text{Cu}_3\text{O}_{6.95}$ up to 24 T.

We gratefully acknowledge useful discussions with G. Crabtree, M. Fogelström, K. Poeppelmeier, D. Rainer, H. Safar, Y. Song, and S.-K. Yip. We are particularly thankful to C. Hammel for providing the sample. This work was supported by the National Science Foundation (DMR 91-20000) through the Science and Technology Center for Superconductivity. The work at the National High Magnetic Field Laboratory was supported by the National Science Foundation under Cooperative Agreement No. DMR95-27035 and the State of Florida. M.E. acknowledges support from the Deutsche Forschungsgemeinschaft.

*Present address: National High Magnetic Field Laboratory, Tallahassee, FL 32310.

†Present address: University of North Carolina at Chapel Hill, Chapel Hill, NC 27599.

¹U. Welp, W. K. Kwok, G. W. Crabtree, K. G. Vandervoort, and J. Z. Liu, *Phys. Rev. Lett.* **62**, 1908 (1989); U. Welp, S. Fleshler, W. K. Kwok, R. A. Klemm, V. M. Vinokur, J. Downey, B. Veal, and G. W. Crabtree, *ibid.* **67**, 3180 (1991); M. H. Lee, N. Tea, Y.-Q. Song, W. P. Halperin, J. Thiel, M. A. Kennard, K. R. Poeppelmeier, M. M. Fang, and U. Welp, *Physica C* **201**, 95 (1992).

²W. C. Lee, R. A. Klemm, and D. C. Johnston, *Phys. Rev. Lett.* **63**, 1012 (1989).

³W. K. Kwok, J. Fendrich, S. Fleshler, U. Welp, J. Downey, and G. W. Crabtree, *Phys. Rev. Lett.* **72**, 1092 (1994).

⁴M. Roulin, A. Junod, and E. Walker, *Science* **273**, 1210 (1996); M. Roulin, A. Junod, A. Erb, and E. Walker, *Phys. Rev. Lett.* **80**, 1722 (1998); A. Schilling, R. A. Fisher, N. E. Phillips, U. Welp, W. K. Kwok, and G. W. Crabtree, *ibid.* **78**, 4833 (1997).

⁵A. P. Reyes, X. P. Tang, H. N. Bachman, W. P. Halperin, J. A.

Martindale, and P. C. Hammel, *Phys. Rev. B* **55**, R14737 (1997); H. N. Bachman, A. P. Reyes, V. F. Mitrović, W. P. Halperin, A. Kleinhammes, P. Kuhns, and W. G. Moulton, *Phys. Rev. Lett.* **80**, 1726 (1998).

⁶M. Takigawa, P. C. Hammel, R. H. Heffner, and Z. Fisk, *Phys. Rev. B* **39**, 7371 (1989).

⁷A. P. Reyes, H. N. Bachman, and W. P. Halperin, *Rev. Sci. Instrum.* **68**, 2132 (1997).

⁸M. Randeria and A. A. Varlamov, *Phys. Rev. B* **50**, 10 401 (1994).

⁹P. Fulde and S. Strässler, *Phys. Rev. B* **1**, 3017 (1970).

¹⁰V. F. Mitrović, H. N. Bachman, W. P. Halperin, M. Eschrig, J. A. Sauls, A. P. Reyes, P. Kuhns, and W. G. Moulton, *Phys. Rev. Lett.* **82**, 2784 (1999).

¹¹M. Eschrig, D. Rainer, and J. A. Sauls, *Phys. Rev. B* **59**, 12 095 (1999).

¹²M. C. Schabel, C. H. Park, A. Matsuura, Z. X. Shen, D. A. Bonn, R. X. Liang, and W. N. Hardy, *Phys. Rev. B* **55**, 2796 (1997); A. M. Cucolo, R. DiLeo, A. Nigro, P. Romano, F. Bobba, E. Bacca, and P. Prieto, *Phys. Rev. Lett.* **76**, 1920 (1996).